Journal of Physics: Conference Series **123** (2008) 012011 doi:10.1088/1742-6596/123/1/012011

Comparison of the spatial and temporal structure of type-I ELMs

A Kirk[1], N Asakura[2], J A Boedo[3], M Beurskens[1], G F Counsell[1], T Eich[4], W Fundamenski[1], A Herrmann[4], Y Kamada[2], A W Leonard[5], S Lisgo[1], A Loarte[6], N Oyama[2], R A Pitts[7], A Schmid[4] and H R Wilson[8]
for the Pedestal and Edge Physics ITPA Topical Group

1 Euratom/UKAEA Fusion Association, Culham Science Centre, Abingdon, UK
2 Naka Fusion Research Establishment, Japan Atomic Energy Research Institute, Ibaraki, Japan
3 Center for Energy Research Eng. University of California, Building Unit II, 9500 Gilman Dr, La Jolla, CA 92093-0417, USA
4 Max-Planck-Institut fur Plasmaphysik, EURATOM Association, Garching, Germany
5 General Atomics, PO Box 85608, San Diego, CA, 92186-5608, USA
6 EFDA Close Support Unit—Garching, 2 Boltzmannstrasse, Garching, Germany
7 Centre de Recherches en Physique des Plasmas, Association Euratom Confedereration Suisse, Ecole Polytechnique, CH-1015 Lausanne, Switzerland
8 University of York, Heslington, York YO10 5DD UK

E-mail: Andrew.kirk@ukaea.org.uk

Abstract: A comparison of the spatial and temporal evolution of the filamentary structures observed during type I ELMs is presented from a variety of diagnostics and machines. There is evidence that these filaments can be detected inside the LCFS prior to ELMs. The filaments do not have a circular cross section instead they are elongated in the perpendicular (poloidal) direction and this size appears to increase linearly with the minor radius of the machine. The filaments start off rotating toroidally/poloidally with velocities close to that of the pedestal. This velocity then decreases as the filaments propagate radially. By comparing the results from all measurements and from comparison with models it is most likely that the filaments have at least their initial radial velocity when they are far out into the SOL and before they have interacted with the nearest limiter surface. There is a general consensus that the dominant loss mechanism in the separated filaments is through parallel transport and that the transport to the wall is through the radial propagation of these filaments. Measurements of the filament energy content show that each filament contains up to 2.5 % of the energy released by the ELM at the time it separates from the LCFS, assuming $T_i = T_e$. The parallel flux e-folding length measured on DIII-D, AUG and MAST has a weaker scaling with normalised ELM size than appears to be necessary to explain the deficit in the ELM energy arriving in the divertor on JET, assuming a purely exponential decay of the filament energy with time.

1. Introduction

Extrapolations for the amount of energy released by Type I Edge Localised Modes (ELMs) in ITER, based on data from existing tokamaks, indicate that the largest ELMs could not be tolerated regularly because of the damage they would cause [1]. However, there is considerable uncertainty associated with such predictions because of the lack of understanding of all of the processes involved. If the understanding of at least some aspects of the ELM event can be improved, it would mean that models could be further constrained and a reduction in the uncertainty of the predictions for ITER obtained.

Filament structures have been observed during ELMs in a wide range of Tokamaks using a variety of diagnostics (see [2] and references therein). In reference [3] a compilation of the radial size and propagation of these filaments was produced. It was found that the radial velocity varied widely across devices as well as in a single device, highlighting the fact that although it is clear that filament structures exist during the ELM, it is still unclear which parameters determine their size and how they propagate. Similar to reference [4], it is proposed in this paper that the ELM evolution can be broken down into three distinct phases: 1) the linear growth stage of the mode resulting in localised structures inside the Last Closed Flux Surface (LCFS), 2) the rapid growth and formation of filaments that extend outside the LCFS and 3) the separation of these filaments from the core and their radial motion towards the first wall/limiters. It is in the third stage of this process, when there is a clear gap between the plasma in the filament and the core plasma that energy and particles are transported to the walls.

The layout of this paper is as follows: in section 2 the evidence for precursor activity related to the growth of the filaments will be discussed. In section 3 and 4 a review of the size and motion of the filaments will be presented. In section 5 the energy content of the filaments will be discussed and in section 6 a study of the dependence of the power e-folding length on plasma parameters will be presented.

2. The linear growth stage and pre-cursor activity

The peeling-ballooning mode theory is now widely accepted as the explanation for the observed pressure limit prior to an ELM [5]. This model predicts that Type I ELMs in tokamaks will onset due to an instability with a toroidal mode number in the range 3-40 [6]. Several Type I ELM precursors, consistent with predictions of this model, are observed using a range of techniques as illustrated below.

On ASDEX Upgrade an ELM precursor signal is detected in the electron temperature from Electron Cyclotron Emission (ECE) channels resonant within the pedestal region. The precursor has a broad spectrum around $f \sim 5$ kHz [7] starting ~ 500 μs before the ELM onset. In JT-60U 200-500 μs before an ELM a mode at 5-25 kHz is observed in the reflectometer signal originating just inside the LCFS [8]. On MAST periodic excursions in the interferometer line integral density trace have been observed prior to an ELM [9]. These structures have a frequency of 20-30 kHz and are found to pre-exist the appearance of filaments in the fast camera images. These excursions have a toroidal mode number (n = 10-20), which is similar to that obtained from the camera images when the filaments become visible. There is evidence that these structures start off broad and become narrower as they push out of the plasma and become visible [9]. Further evidence for a structure inside the LCFS prior to the ELM comes from beam emission spectroscopy measurements on DIII-D. This shows evidence for a poloidally and radially localised structure rotating in the poloidal direction [10].

In summary, there is clear evidence for localised structures that exist inside and close to the LCFS that occur just before the onset of an ELM. From the mode number and size of these structures it seems reasonable to assume that these are the precursors to the filament structures that appear at the ELM onset. The characteristics of these filaments will now be discussed in the following sections.

3. Filament size

One of the original pieces of evidence for the toroidal/poloidal non-uniformity of ELMs came from the peaks observed in the ion saturation current (I_{SAT}) measured during an ELM using reciprocating Langmuir probes. A typical signal from ASDEX Upgrade is shown in figure 1. As can be seen, the I_{SAT} signal shows four or more distinct features for one single ELM as observed by the D_α signal. Each

peak lasts for δt~ 50-80 μs and they are separated by Δt~ 100 μs. Similar features have been observed in the ion saturation current on other devices and are summarised in table 1. In reference [11] it was shown that as the toroidal velocity of the plasma increases the width and separation of the filaments decrease hence allowing an interpretation of the peaks as localised structures rotating past the probe. It has subsequently been confirmed by correlating visible images with the I_{SAT} data that the peaks are due to the interaction of moving filaments with the probe [12]. If the radial and/or toroidal/poloidal velocity of the filaments is known then the width and separation of the peaks can be used to estimate the size and quasi-mode number of the filaments. Table 1 shows how device dependent assumptions have been made leading to different estimates for the size of the filaments.

Table 1 Measurements of the temporal width (δt) and separation (Δt) of peaks observed in ion saturation current traces during ELMs on a variety of devices. These measurements have been combined with toroidal (V_ϕ) or radial (V_r) velocities to estimate the size (δ) and mode number of the filaments.

Device	δt (μs)	Δt (μs)	Velocity used (kms^{-1})	Size (cm)	Mode number	Ref.
AUG	50-80	100-200	$V_\phi = 10$	$\delta_\perp = 8$-13	10-20	[2]
DIII-D	50-100	150-250	$V_\phi = 13$	$\delta_\perp = 8$-16	10	[10]
MAST	15	60	$V_\phi = 10$	$\delta_\perp = 7$	10-20	[11]
NSTX	10	20-50	$V_\phi = 10$	$\delta_\perp = 7$	5-15	
JET	100-150	300	$V_\phi = 80$	$\delta_\perp = 100$	2	
			V_ϕ/(5–10)	$\delta_\perp = 10$-20	10-20	[13]
	185		$V_r = 0.7$	$\delta_r \leq 8$		[14]
JT-60U	10-25		$V_r = 0.5$-1.5	$\delta_r = 0.5$-4		[15]
			$V_\phi = 30$	$\delta_\perp = 4$-10		

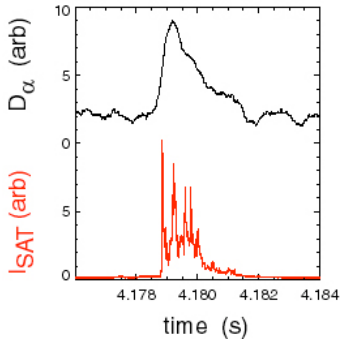

Figure 1 The target D_α and mid-plane ion saturation current during an ELM on ASDEX Upgrade.

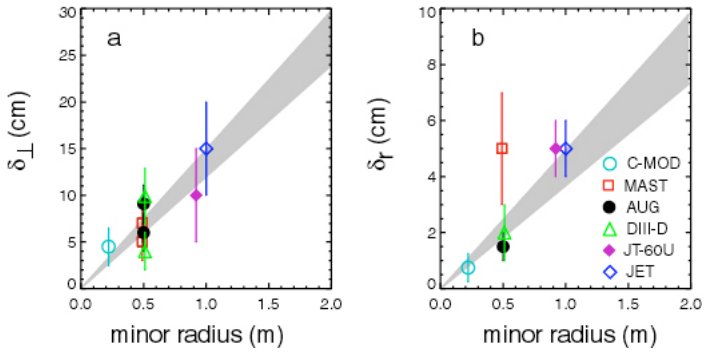

Figure 2 The a) perpendicular and b) radial size of the filaments as a function of machine minor radius. The shaded area represents the ±1σ region of a fit to the data. In b) the open square (MAST data) has been omitted from the fit.

As can also be seen from figure 1, the I_{SAT} signal is composed of several peaks which are superimposed on top of a base level that begins after the first peak. This base level follows the general trend of the D_α signal suggesting it is related to the particles being released into the SOL due to the ELM. The peaks are observed for up to 1ms, much longer than the time for the pedestal losses to occur. Similar long pulse trains of peaks are observed in the I_{SAT} data from DIII-D [10] and JET [13].

However, on MAST, which has a large gap to the first wall/limiter, the length of time that peaks are observed for is much shorter, typically 100-150 μs. This raises the question of the effect of the wall on the filaments. In fact recent results from ASDEX Upgrade have shown that secondary filaments can be produced when the original filaments impact with the limiter [16].

It has been noted in JET [14] and MAST [17] that the temporal width of the I_{SAT} peaks increases with distance from the LCFS. In reference [14] it was argued that this was due to the dispersion of the filament, however, as will be shown below it is possibly due to the fact that the toroidal/poloidal motion of the filament decreases as it expands away from the LCFS.

Direct evidence for the size of the filaments has come from a variety of sources, including, visible and infrared imaging, Thomson Scattering and beam emission spectroscopy; the results are summarised in table 2. The size of the filament in the radial direction is denoted as δ_r and $\delta_\perp$ is defined as the size perpendicular to both the field line and the radial direction. In all cases the radial extent is smaller than the perpendicular extent. The mode numbers are similar to those derived from the I_{SAT} measurements, however, the observed perpendicular widths tend to be smaller.

Although there is a large spread in the data, these are the only data available in order to make extrapolations to future devices such as ITER. Figure 2a plots the measured perpendicular size of the filaments ($\delta_\perp$) as a function of minor radius. Although there is a large spread in the values the data are consistent with an increase in size with increasing machine. A linear fit has been performed to the data and the shaded area represents the $\pm 1\sigma$ region, which can be used to predict filament sizes on ITER of between 23 and 30 cm. Figure 2b is a plot of the radial filament size (δ_r) with minor radius. Obtaining a simple scaling with minor radius is not so simple here since the radial extent on MAST is larger than that on AUG and DIII-D but similar to that on JET and JT-60U. However, if the results from MAST (open square) are excluded by arguing that the magnetic geometry is different on a spherical tokamak then it is possible to extract a linear fit to the remaining data, which would indicate that the filaments would have a radial extent of between 7 and 10 cm on ITER.

Table 2 Measured radial (δ_r) and perpendicular ($\delta_\perp$) filament sizes from a variety of diagnostics and devices.

Device	Method used	δ_r (cm)	$\delta_\perp$ (cm)	Mode Number	Ref.
AUG	TS	1-2	6		[18]
	IR outer limiter		2-6		[19]
	Visible		5-8	10-20	[2]
	RP Mag	1	3		[20]
C-MOD	Visible	0.5-1	> 4.5		[21]
DIII-D	BES	> 2	2-4		[10]
	Visible			18	[22]
MAST	TS	4-6			[9]
	Visible		3-7	10-20	[23]
JET	TS	4-5			[24]
	IR outer limiter		10-20	11-16	[25]
JT-60U	Visible	3-5			[15]

4. Filament propagation

The poloidal/toroidal motion of the filaments determines the region of interaction of the filaments with the first wall/limiter, while their radial motion, energy content and loss mechanism determine the magnitude of the interaction. There is a general consensus about the loss mechanism for the filaments: the electrons cool more rapidly than the ions and the density is removed by ion parallel processes. This is based on a number of observations, including: 1) that the divertor ELM energy flux rise time is

correlated with the ion transport time [26], 2) that the particle content of the filaments decreases exponentially with distance from the LCFS and 3) that the electron temperature in the filament decreases more rapidly [10] than the ion temperature [13][27].

Initial studies of the toroidal and poloidal velocity during a Type I ELM were made from measurements of the edge rotation using Charge Exchange Recombination spectroscopy on DIII-D [28] and helium Doppler spectroscopy on MAST [11]. In both cases a rapid drop in the edge rotation is observed during the rise time of the D_α light associated with the ELM. The measurements are obtained using an integration time which is long (270 μs DIII-D, 125 μs MAST) compared to the filament lifetime, so it is not possible to determine from these measurements alone if it is the filaments and/or the bulk plasma which is slowing down.

Table 3 Measurements of the radial (V_r) and toroidal velocity (V_ϕ) of the filaments from a variety of diagnostics and devices.

Device	Method	$<Vr>$ (kms^{-1})	V_ϕ (kms^{-1})	Comments	Ref.
AUG	$t(J_{SAT}\,peak)$- $t(D_\alpha)$	0.4		Vr increases with Δ_r	[2]
	$t(probe_1)$- $t(probe_2)$		10-20	Decreases during ELM	[20]
	$t(probe_1)$- $t(probe_2)$	> 1		Even for large Δ_r	[20]
	TS	0.8			[18]
	Visible				
C-MOD	Visible	1-2		Later filaments slower	[21]
DIII-D	$E \times B$	0.2-0.6		Decreasing with Δ_r	[10]
	BES	8		V_r at filament ejection	[10]
	Reflectometer	0.5			[31]
	Divertor tile currents		13.5		[10]
	CER		40	Decreases with t and Δ_r	[28]
MAST	Visible	1-9		Increases with t and Δ_r	[23]
			25-0	Decreases with t and Δ_r	[23]
	CER		20-5	Decreases with t and Δ_r	[11]
	TS	8			[29]
NSTX					
JET	$t(probe_{lim})$ –$t(D_\alpha)$	0.7			[14]
	$t(probe_{RP})$ –$t(D_\alpha)$	0.75			[32]
	$E \times B$	1-2		Decreases with f_{ELM}	[33]
JT-60U	$t(J_{SAT}\,peak)$- t_0	0.4-2.9		Increases with Δ_r	[15]

Direct observation of the toroidal motion of the filaments has been reported on MAST using fast visible imaging [29] [30]. These show that the filaments start off at the plasma edge rotating at the velocity of the pedestal. After 50-100 μs, the filaments decelerate toroidally and accelerate radially outwards. As the filaments propagate radially they follow the direction of the local field line and remain approximately constant in width ($\delta_\perp$). Similar observations have recently been repeated on ASDEX Upgrade [16]. Filaments are observed, which start off rotating toroidally in the co-current direction and after sometime the toroidal rotation of an individual filament slows and soon afterwards it hits the limiter (12 cm from the LCFS). Although it is not possible to directly track the radial position of the filaments they are observed for up to 60 μs before hitting the limiter (12 cm distant), which gives a lower limit of the mean radial velocity of 2 kms^{-1}.

The measurements of the toroidal/poloidal and radial velocities from all devices are summarised in table 3. As can be seen in all devices, where data are available, agree that the filaments rotate initially with velocities near to the pedestal values and then decrease with time and distance into

the SOL. Where there is more disagreement is in the radial propagation. For example, on MAST it is claimed from an analysis of the visible images that the filaments accelerate away from the edge but on DIII-D measurements of the electric field indicate that the filaments decelerate.

The radial propagation of the filaments has been determined by a number of techniques and it is interesting to look at the difficulties of each. For example, on MAST, initial estimates of the radial velocity were made using the time difference between the start of the rise time of the D_α light and the peak in the I_{SAT} at the mid-plane reciprocating probe as a function of distance from the LCFS [17]. A higher statistics analysis [11] showed that the data were in fact consistent with the velocity increasing with distance and hence compatible with the filaments moving radially with accelerations in the range (0.5-1.5) x10^7 ms^{-2}. Due to the large shear in the magnetic field at the outboard mid-plane on MAST, the pitch angle of the field line changes rapidly with distance from the LCFS and hence it is possible to determine the radial location of the filaments to within 1cm [29]. This radial location accuracy was cross checked by tracking filaments until they interacted with the reciprocating probe placed at various distances from the LCFS. Analysis of the image data again showed that the velocity of the filaments increased with distance from the LCFS, but in this case the accelerations were in the range (0.7-2.5)x10^8 ms^{-2} [23]. The images reveal that the reason for the discrepancy between the two results is due to the fact that the filaments do not all leave the LCFS at the same time and they do not begin to separate until 50-100 μs after the start of the rise in the D_α light. Hence the propagation time to the probe was over estimated in the I_{SAT} analysis and the subsequent velocity/acceleration underestimated.

A similar effect is seen in the ASDEX Upgrade data in that the mean radial velocity calculated using the difference between the peak in the I_{SAT} and the start in the rise of the D_α light [2] is smaller than the velocity calculated using the difference in time between two radially separated probes [20].

On DIII-D, the radial velocity of the ELM filaments has been determined from measurements of the poloidal electric field (E_θ) and using $V_r = E_\theta B / B^2$. This shows that the velocity decreases from ~ 500 ms^{-1} at the LCFS to ~ 120 ms^{-1} near the wall (4 cm from the LCFS) [10]. This is in sharp contradiction with the velocities of > 1 kms^{-1} at distances greater than 10 cm on MAST, ASDEX Upgrade and JT-60U (see table 3) The difference could be due to the difficulties of measuring the electric field in the ELM filaments or due to the fact that the radial velocity is not simply driven by $E \times B$ or because the wall/limiter may have an influence on the dynamics [16].

5. Energy content of the filaments

In order to make a quantitative prediction for the amount of power arriving outside the divertor, in addition to the information on the size and motion of the filament, a knowledge of how much energy is in the filament at the time it separates from the LCFS is needed. In order to measure the energy content of the filament the density, electron and ion temperatures and the filament volume are required. On MAST the radial density and electron temperature profiles of filaments, obtained from Thomson scattering, have been combined with the measured perpendicular size and the assumption that the filament extends between upper and lower X-points to calculate the energy content assuming $T_i = T_e$ [9] (although as discussed below T_i ~2-3T_e may be a better assumption). The maximum energy content of a single filament, observed close to the LCFS, is 2.5 % of ΔW_{ELM}. Recently filament structures have been observed in the Thomson scattering radial profiles on JET [24]. In the cases reported the maximum energy content of a filament is 2 kJ from an ELM with ΔW_{ELM} = 100 kJ. These observations would suggest that the maximum amount of ELM energy transported to the wall would be 25 % ($T_i = T_e$) or 50 % ($T_i = 3T_e$) for 10 filaments. Note that this assumes all the filaments have the maximum size observed and hence is likely an over estimate.

6. Parameters effecting the radial evolution

Rather than reporting individual filament motion the radial expansion of the filaments is often captured in terms of a radial e-folding length of particles and energy. In the simplest picture where the filaments propagate out radially with a constant velocity (V_r) and lose particles on ion parallel

transport timescales ($\tau_{//} = L_{//}/c_s$, $L_{//}$ is the connection length and c_s the plasma sound speed) then the particle e-folding length (λ) can be expressed as $\lambda \sim V_r\tau_{//} \sim V_r L_{//}/c_s$. Initial evidence that the electron temperature in the ELM filaments decayed rapidly with distance from the LCFS came from reciprocating probe measurements on DIII-D [10]. These results showed that the ELM filament electron temperature is nearly that of the pedestal (400 eV) when it exits the plasma near the LCFS but falls exponentially with a decay length of 1-1.5cm. Measurement of the electron temperatures 4 cm from the LCFS on JET showed that high temperature electrons do not reach this region, the maximum temperature being measured was ~ 40 eV [33]. In contrast, measurements with a retarding field analyser probe on JET have indicated ion temperatures of 100-150 eV [13]. This large ratio of ion temperature to the electron temperature in the far SOL has also been observed on ASDEX Upgrade [27]. The heat flux to the reciprocating probe obtained from infrared measurements has been compared with the corresponding particle flux measured by Langmuir probes in order to estimate ion temperatures of ~ 60 eV.

In order to turn the I_{SAT} values into a measurement of the density of particles in the filaments a knowledge is needed of both the electron and ion temperature. Often in analyses of L-mode plasmas it is assumed that $T_i = T_e$, but as we have noted above this is not true for the ELM filaments. In DIII-D, the density in the filaments was calculated from the I_{SAT} and the measured electron temperature assuming $T_i = T_e$ [10]. The electron density, calculated in this way, was found to fall off more slowly than the electron temperature. In addition the density e-folding length was found to depend on the density of the plasma having $\lambda \sim 3$cm at high density and $\lambda \sim 10$ cm at low density. This was the first indication that the radial efflux could depend on a plasma parameter.

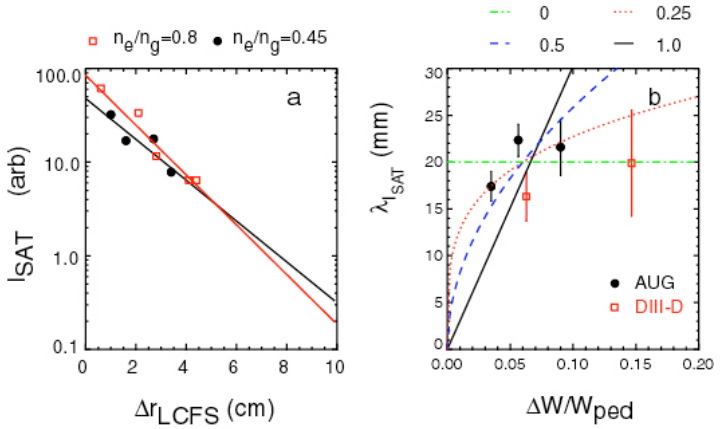

Figure 3 a) The ion saturation current as function of Δr_{LCFS} derived from published data from DIII-D for two shows with different fractional Greenwald (n_g) densities. b) λ_{ISAT} as a function of $\Delta W/W_{ped}$ derived from the data shown in a) and combined with the data from ASDEX Upgrade [16]. The superimposed curves are described in the text.

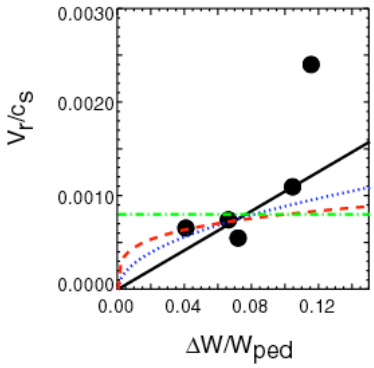

Figure 4 The filament radial velocity measured on DIII-D as a fraction of the ion sound speed as a function of $\Delta W/W_{ped}$. The superimposed curves are described in the text.

In order to determine the power load to the limiters what is needed is the power e-folding length. On ASDEX Upgrade it has been shown that the e-folding lengths in ion saturation current and power are the same [27]. Since it is the ion saturation current that is measured in most experiment, the radial profiles of I_{SAT} have been re-calculated from the published DIII-D density and temperature measurements (see figure 3a). The difference between the I_{SAT} slopes for the low (λ_{ISAT} = 20± 5 mm) and high (λ_{ISAT} = 16 ± 2 mm) density cases is much less pronounced. Using the measured dependence of the fraction of the pedestal energy released by an ELM ($\Delta W_{ELM} / W_{ped}$) on plasma density on DIII-

D [34], the dependence of the e-folding length on ELM size has been calculated. Figure 3b shows a plot of the ion saturation current e-folding length versus the ELM size expressed as a fraction of the pedestal energy. Also shown in figure 3b are recent results from ASDEX Upgrade [16]. It is interesting to note that the e-folding lengths are similar to those observed in DIII-D. Although any dependence of the e-folding length is small compared to the scatter in the underlying data, which is reflected in the error bars, the same trend as in the DIII-D data is observed i.e. a small increase in the e-folding length with $\Delta W_{ELM} / W_{ped}$. Superimposed on the figure are curves of the form: $\lambda \propto (\Delta W / W_{ped})^{\alpha}$ with $\alpha = 0$ (dashed-dot), 0.25 (dashed), 0.5 (dotted) and 1 (solid). From these data it is difficult to rule out any of these dependencies, however, fits with $\alpha = 0.5$ or 1 are strongly disfavoured.

Similar measurements of the ion saturation current e-folding length have been made as a function of $\Delta W_{ELM} / W_{ped}$ on MAST [16]. The curve that gives the poorest description of the data is $\alpha = 1$. If it is assumed that a single value of α should be valid for the dependence of λ_{ISAT} on $\Delta W_{ELM} / W_{ped}$ in DIII-D, ASDEX Upgrade and MAST then the best value of α is 0.25, although no dependence (i.e. $\alpha = 0$) can not be ruled out. In reference [16] it has been suggested that a better fit may be of the form $\lambda = \lambda_{fil} + A.(\Delta W_{ELM} / W_{ped})^{\alpha}$, where λ_{fil} represents the radial size and energy distribution with the filament. The values of λ_{fil} obtained from fits to MAST and ASDEX Upgrade data are at least consistent with the radial size of the filaments being larger in MAST [16].

As was discussed above, on DIII-D the radial expansion velocity of the filaments has been measured using reflectometry [31]. This device measures the velocity of a particular density layer and not explicitly the velocity of the filament. In reference [35] these measurements were collected together and plotted as a function of $\Delta W_{ELM} / W_{ped}$. These data are plotted in figure 4, where curves representing $\frac{V_r}{c_S} \propto \left(\frac{\Delta W}{W_{ped}} \right)^{\alpha}$ with $\alpha = 0$, 0.25, 0.5 and 1 have been superimposed. As can be seen any dependence relies, to a large extent, on the validity of the highest point. A similar scaling has been investigated in MAST using measurements of the radial velocity of the filaments from visible images. In this analysis V_r/c_s is found to be approximately constant with $\Delta W_{ELM} / W_{ped}$ [16].

The interchange instability predicts that more intense filaments travel faster and that $\frac{V_r}{c_s} \sim \sqrt{\frac{2\delta_{\perp} \Delta W}{R W_{ped}}}$ [36]. In reference [37] this parameterisation has been compared with far SOL average power widths, measured by IR, obtained during wall-outer gap scan experiments in JET. Assuming that the filament size ($\delta_{\perp}$) does not change with ELM size, the above parameterisation predicts a scaling for the power e-folding length of $\lambda^{W}_{ELM} \approx 35(\Delta W_{ELM}/0.12 W_{ped})^{0.5}$mm [38]. Note that the dependence of the e-folding length on $\Delta W_{ELM} / W_{ped}$ has not been tested directly, instead it has been used to predict the fraction of ELM energy deposited on the wall, which has been compared with measurements from JET [38][39]. The experimental measurements show that the fraction of ELM energy reaching the divertor approaches unity at small $\Delta W_{ELM} / W_{ped}$ but decreases to ~ 50 % at large values of $\Delta W_{ELM} / W_{ped}$ [38]. In reference [37], a parallel loss model of the ELM filament evolution [4] was used to predict an expression for the energy arriving at the wall (i.e. not arriving at the target) of the form $W_{Wall} / W_0 = \exp[-(\Delta_{ped} / 2 + \Delta_{sol}) / \lambda^{W}_{ELM}]$ where W_0 is the initial energy content of the filament, W_{Wall} the energy deposited on the wall and Δ_{ped} and Δ_{sol} are the radial widths of the pedestal and SOL respectively. The model used in [38], which assumes $W_0 = \Delta W_{ELM}$, agrees with the JET data

for $\Delta W_{ELM} / W_{ped} \geq 0.15$ but predicts a smaller flux to the divertor than is measured for smaller ELMs. In reference [39] it has been shown that a better fit to the data is possible if $\lambda \propto (\Delta W_{ELM} / W_{ped})^{\alpha}$ with $\alpha \geq 1$ is used. However, such large values of α are incompatible with the direct measurements presented in figure 3b.

In summary, direct measurements show that the ion saturation current e-folding lengths depend weakly on the size of the ELM ($\Delta W_{ELM} / W_{ped}$). In contrast, the fraction of energy arriving at the divertor in JET, calculated assuming a purely exponential decay of the filament energy with time (radius), requires both a strong increase in λ with $\Delta W_{ELM} / W_{ped}$ and also that the fraction of energy carried by the filaments is larger than what is measured experimentally. Understanding the reason for these discrepancies should be an urgent task for future experiments.

7. Summary

In this paper a summary of the results on the size and motion of filaments observed during type I ELMs has been presented. There is evidence that these filaments can be detected inside the LCFS prior to ELMs. The size of the filaments has been studied on a variety of devices and there is evidence that the filaments do not have a circular cross section instead they are elongated in the perpendicular (poloidal) direction. The results from all the tokamaks presented are consistent with the perpendicular size increasing linearly with the minor radius of the machine giving an estimate for their size on ITER as $\delta_{\perp}$ = 23-30 cm. Obtaining a scaling for the radial size is more difficult, but the best estimate for ITER, again assuming this scales with the size of the machine, is δ_r = 7-10 cm.

Turning now to the motion of the filaments, there is general agreement that the filaments start off rotating toroidally/poloidally with velocities close to that of the pedestal. This velocity then decreases as the filaments propagate radially. Where there is less agreement is on the radial propagation, however, weighing up all the evidence it is most likely that the filaments have at least their initial velocity when they are far out into the SOL and before they have interacted with the nearest limiter surface. Once the filament interacts with the nearest limiter then it is more difficult to predict its evolution. Whether the filaments travel with a constant velocity or accelerate away from the LCFS needs data from other devices.

There is a general consensus that the dominant loss mechanism is through parallel transport and the transport to the wall is through the radial propagation of these filaments. Measurements of the filament energy content show that each filament contains up to 2.5 % of the energy released by the ELM at the time it separates from the LCFS and it would appear that the dominant energy loss has occurred while the filaments are still attached to the LCFS [30]. Finally, the parameters that determine this radial propagation and how this effects the power e-folding length and hence the power loading to non-divertor components have been discussed. The ion saturation current e-folding lengths, which are assumed to represent the power e-folding lengths [27], show a weak, if any, dependence on $\Delta W_{ELM} / W_{ped}$. The dependence that best fits the data, if there is any dependence at all, is $\lambda^{W}{}_{ELM} \propto (\Delta W_{ELM} / W_{ped})^{\alpha}$ with α = 0.25. However, measurements of the fraction of energy arriving at the divertor require larger values of α and larger energy content of the filament, particular at larger values of $\Delta W_{ELM} / W_{ped}$.

Acknowledgement

UKAEA authors were funded jointly by the United Kingdom Engineering and Physical Sciences Research Council and by the European Communities under the contract of Association between EURATOM and UKAEA. The views and opinions expressed herein do not necessarily reflect those of the European Commission.

References

[1] Loarte A *et al*. 2002 *Plasma Phys. Control. Fusion* **44** 1815
[2] Kirk A *et al*. 2005 *Plasma Phys. Control. Fusion* **47** 995
[3] Lipshultz B *et al*. 2007 *Nucl. Fusion* **47** 1189
[4] Fundamenski W and Pitts R A 2006 *Plasma Phys. Control. Fusion* **48** 109
[5] Connor J W *et al*. 1998 *Phys. Plasmas* **5** 2687
[6] Snyder P B *et al*. 2004 *Plasma Phys. Control. Fusion* **46** A131
[7] Suttrop W *et al*. 1996 *Plasma Phys. Control. Fusion* **38** 1407
[8] Oyama N *et al*. 2004 *Nucl. Fusion* **44** 582
[9] Scannel R *et al*. 2007 *Plasma Phys. Control. Fusion* **49** 1431
[10] Boedo J A et al. 2005 *Phys. Plasmas* **12** 072516
[11] Kirk A *et al*. 2005 *Plasma Phys. Control. Fusion* **47** 315
[12] Kirk A *et al*. 2006 *Plasma Phys. Control. Fusion* **48** B433
[13] Pitts R A *et al*. 2006 *Nucl. Fusion* **46** 82
[14] Fundamenski W *et al*. 2004 *Plasma Phys. Control. Fusion* **46** 259
[15] Asakura N *et al*. 2006 *Proc of 21st IAEA Fusion Energy Conf., (Chengdu)* IAEA-CN-149/EX9-2
[16] Kirk A *et al*. 2007 'Comparison of the spatial structure of type I ELMs in ASDEX Upgrade and MAST' *this conference*
[17] Kirk A *et al*. 2004 *Plasma Phys. Control. Fusion* **46** 551
[18] Kurzan B *et al*. 2005 *Phys. Rev. Lett.* **95** 145001
[19] Herrmann A *et al*. 2004 *Plasma Phys. Control. Fusion* **46** 971
[20] Schmid A *et al*. 2007 *Proc. 34th EPS conf. on Plasma Physics and Controlled Fusion (Warsaw)* P1-026
[21] Terry J L *et al*. 2007 *J. Nucl. Mater.* **363-365** 994
[22] Fenstermacher M *et al*. 2004 *Proc of 20th IAEA Fusion Energy Conf. (Villamora)* IAEA-CN-116 /EX2-5Rb
[23] Kirk A *et al*. 2004 *Plasma Phys. Control. Fusion* **46** A121
[24] Beurskens M *et al*. paper in preparation.
[25] Andrew P *et al*. 2007 *Proc. 34th EPS conf. on Plasma Physics and Controlled Fusion* I1-005.
[26] Eich T *et al*. 2005 *J. Nucl. Mater.* **337-339** 669
[27] Herrmann A *et al*. 2007 *J. Nucl. Mater.* **363-365** 528
[28] Wade M *et al*. 2005 *Phys. Rev. Lett.* **94** 225001
[29] Kirk A *et al*. 2006 *Phys. Rev. Lett.* **96** 185001
[30] Kirk A *et al*. 2007 *Plasma Phys. Control. Fusion* **49** 1259
[31] Zeng L *et al*. 2007 *Plasma Phys. Control. Fusion* **49** 1259
[32] Gonzales B *et al*. 2003 *Plasma Phys. Control. Fusion* **45** 1627
[33] Silva C *et al*. 2005 *J. Nucl. Mater.* **337-339** 722
[34] Leonard A W *et al*. 2003 *J. Nucl. Mater.* **313-316** 768
[35] Loarte A *et al*. 2006 *Proc of 21st IAEA Fusion Energy Conf, (Chengdu)* IAEA-CN-149/IT/P1-14
[36] Garcia O E *et al*. 2006 *Physics of Plasmas* **13** 082309
[37] Fundamenski W and Pitts R A 2007 *J. Nucl. Mater.* **363-365** 319
[38] Pitts R A *et al*. 2006 *Proc of 21st IAEA Fusion Energy Conf. (Chengdu)* IAEA-CN-149/EX/3-1
[39] Eich T et al. 2007 *Plasma Phys. Control. Fusion* **49** 573